Scanning force microscopy characterization of individual carbon nanotubes on electrode arrays

J. Muster,[a] M. Burghard, and S. Roth
Max-Planck-Institut für Festkörperforschung, Heisenbergstr. 1, D-70569 Stuttgart, Germany

G. S. Duesberg
Department of Physics, Trinity College Dublin, Dublin 2, Ireland

E. Hernández and A. Rubio
Departamento Fisica Teorica, Universidad de Valladolid, 47011 Valladolid, Spain

(Received 6 March 1998; accepted 12 June 1998)

We report the controlled adsorption of individual multi- and single-walled carbon nanotubes from purified aqueous dispersions onto chemically modified silicon oxide surfaces as well as on predefined electrode patterns (100 nm electrode separation). Detailed structural investigations were performed using scanning force microscopy (SFM) without interference from other carbon materials. These studies revealed the striking flexibility of single-walled nanotubes. In contrast to comparably stiff multi-walled nanotubes (MWNTs) which bridged the electrode lines, single-walled nanotubes (SWNTs) were found to follow the profile of the underlying electrodes almost exactly. Based upon the SFM cross sectional analysis of an individual MWNT (8 nm diameter) a Young modulus of about 1 TPa was estimated. Furthermore, nanotube adsorption from the surfactant-stabilized dispersions led to flow-induced orientation processes. © *1998 American Vacuum Society*. [S0734-211X(98)00605-2]

I. INTRODUCTION

Since their discovery in 1991,[1] carbon nanotubes (NTs) have been investigated intensively because of their outstanding electronic and mechanical properties. Many applications have been proposed including hydrogen storage,[2] field emission[3] or electrical devices.[4,5] The electronic structure of individual SWNTs is of especially great interest, because theory predicts different electrical behavior (metallic or semiconducting) depending on the diameter and wrapping angle of the tube.[6] Electrical transport studies on NT ropes or individual NTs revealed single-electron tunneling[7] and rectifying behavior.[8] Furthermore, SWNTs have been shown to behave like quantum wires at low temperatures.[9]

A number of theoretical studies[10,11] have predicted NTs to be extraordinarily resilient, being able to sustain extreme strain without any irreversible deformation or other damage. The elastic properties are highly anisotropic:[12] the tubes are stiff parallel to their axial direction, but flexible perpendicular to it. Therefore NTs may find applications in new composite materials[13] or as stable and sharp probes in scanning force microscopy (SFM).[14]

Different characterization methods have been applied to NTs. With scanning electron microscopy (SEM) one can easily observe multi-walled nanotubes. In contrast, SWNTs are hard to detect using this technique due to their low height and material contrast. In addition, SEM is a destructive method: deposition of carbon material[15] or even damage of the tubes may occur. Transmission electron microscopy (TEM) is an excellent high resolution technique for imaging of NTs, but requires transparent substrates. In contrast, scanning probe microscopy techniques combine high resolution (down to atomic features) with real three-dimensional imaging and are therefore excellent methods for structural investigations of NTs. Scanning force microscopy also allows measurement of the mechanical properties of the NT samples.[16,17]

Reliable studies of the electrical properties of NTs strongly depend on tube material of high purity. Recently, we reported a nondestructive purification method using size exclusion chromatography.[18] This procedure is applicable to surfactant-stabilized aqueous dispersions of both, single- and multi-walled nanotubes. In this article, we present SFM studies of individual SWNTs and MWNTs deposited from such purified dispersions on chemically modified wafer surfaces as well as on electrode arrays. One aim was to investigate the dependence of adsorption characteristics of micellar dispersed NTs on the chemical nature and topography of the substrate surface. We also investigate the mechanical flexibility of individual multi- and single-walled NTs, which is important for an understanding of future electrical measurements.

II. SAMPLE PREPARATION AND METHOD

MWNTs were prepared by the conventional arc-discharge method.[19] The SWNTs were synthesized in an arc plasma in the presence of a Ni-Y catalyst.[20]

Silicon wafers with a 1 μm thick thermally grown oxide layer were used as substrates. Electrode patterns (Au/Pd 3/2) were formed by conventional e-beam lithography using a double layer PMMA resist and a modified Hitachi S2300 microscope.

[a]Electronic mail: muster@klizix.mpi-stuttgart.mpg.de

As reported previously, MWNTs and SWNTs were dispersed in water with the aid of sodium dodeclysulfat (SDS) and subjected to size exclusion chromatography.[18] The purified NTs were then directly deposited on chemically modified SiO_2 surfaces.[21] The wafers were treated with an aqueous 2,5 mmol/l 3-aminopropyltriethoxysilane (APS) solution for 15 min at room temperature in order to create positively charged amino groups on the SiO_2 surface. Substrates with electrodes obtained from e-beam lithography were used without any further chemical modification. Adsorption times of the NT fractions depended on their concentration and ranged typically between 15 and 30 min. The surfactant was removed by a brief rinse with pure water, followed by drying of the substrate in air.

Scanning force microscopy was performed with a Nanoscope IIIa system (Digital Instruments), using a MultiMode base and 14 μm E-Scanner. All measurements were carried out under ambient conditions. Samples were investigated in Tapping Mode, using commercial silicon cantilevers (Nanoprobe).

III. IMAGING OF INDIVIDUAL NANOTUBES ON CHEMICALLY MODIFIED SUBSTRATES

First, experiments were performed on substrates without electrodes in order to evaluate sample homogeneity, appropriate adsorption times and the structural integrity of the tubes. Figure 1 presents two SFM images of MWNTs adsorbed from micellar dispersions before and after chromatographic separation, respectively. Figure 1(a) demonstrates that the unpurified material consists of thick rods (bundles of MWNTs) and larger particles (presumably polyhedra and amorphous carbon), which are partially interconnected. In the present case, the surface was not rinsed with water and consequently the tubes are still embedded in a sea of surfactant, which is visible as a smooth gray background in contrast to the dark wafer surface. Figure 1(b), corresponding to the adsorbed purified tubes after rinsing with water, illustrates the presence of well-distinguished individual MWNTs, to which no or only few particles are attached. It is noteworthy that the tube lengths in this sample (0.5–1.5 μm) are considerably smaller than those of the unpurified sample ($<$0.1–5 μm). This result is related to size separation during the chromatographic process[18] and could be confirmed by SFM measurements on MWNTs adsorbed from various chromatographic fractions. Similar behavior occurs in the case of SWNTs adsorbed from surfactant-stabilized dispersions.

In the case of purified samples, it was possible to characterize individual carbon nanotubes in detail without interference from other carbon materials. As a representative example, Fig. 2(a) shows a single MWNT, which is about 1 μm long and 7 nm high. The best measurement of the tube diameter is obtained from the height measurement [bottom of Fig. 2(a)]. The larger apparent width ($\approx$40 nm) of the tube in Fig. 2(a) can be attributed to the convolution of the SFM tip and the measured object.[22] The tip radius of the cantilever can be approximated as follows:[23] the apparent

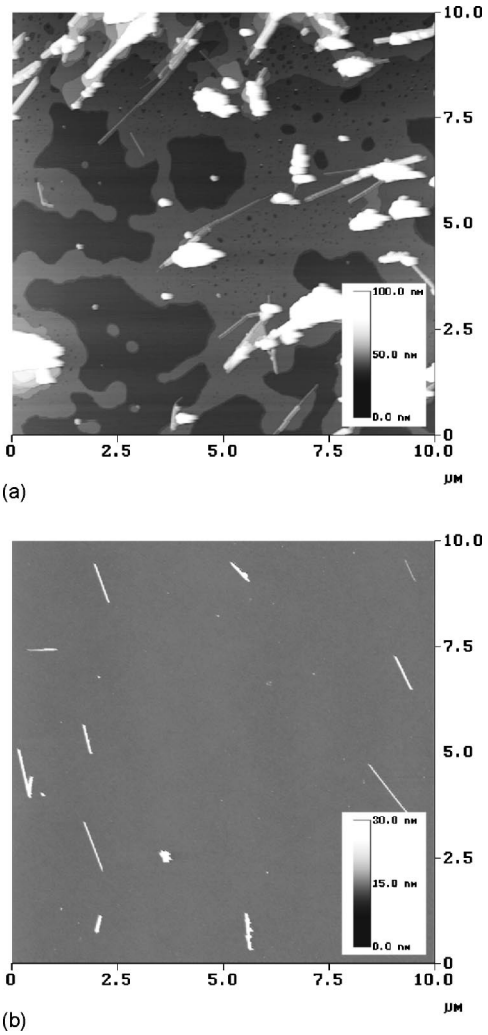

FIG. 1. SFM images of MWNTs adsorbed on APS-treated SiO_2 surfaces (a) before and (b) after chromatographic separation. Only sample (b) was rinsed with water to remove the surfactant.

width w of spherical particles depends on the tip radius r_t and on the radius of the particle r_p according to

$$w = 2[(r_t + r_p)^2 - (r_t - r_p)^2]^{1/2}. \quad (1)$$

From $w \approx 40$ nm and $r_p \approx 3.5$ nm, the tip radius r_t is estimated to be $\approx$30 nm, a value which is reasonable for the pyramidal shaped cantilevers used in the present study (nominal tip radius r_t between 15 nm and 30 nm).

A typical example of an individual single-walled nanotube (approximately 1.2 μm long, 1.1 nm high) is displayed in Fig. 2(b); again the apparent width of 22 nm is enlarged due to tip convolution. The high flexibility of the SWNT is remarkable: in contrast to the rigid, straight MWNTs shown in Fig. 1(b) and Fig. 2(a), the SWNT reveals a distinct curvature. Upon closer inspection of Fig. 2(b), it is recognized that the height of the top end (4 nm) of the tube is slightly larger. This is attributed to the presence of several NTs connected together forming a rope in this end region. The formation of ropes in SWNTs synthesized via the arc-discharge method is well documented.[20] Generally, we interpreted ob-

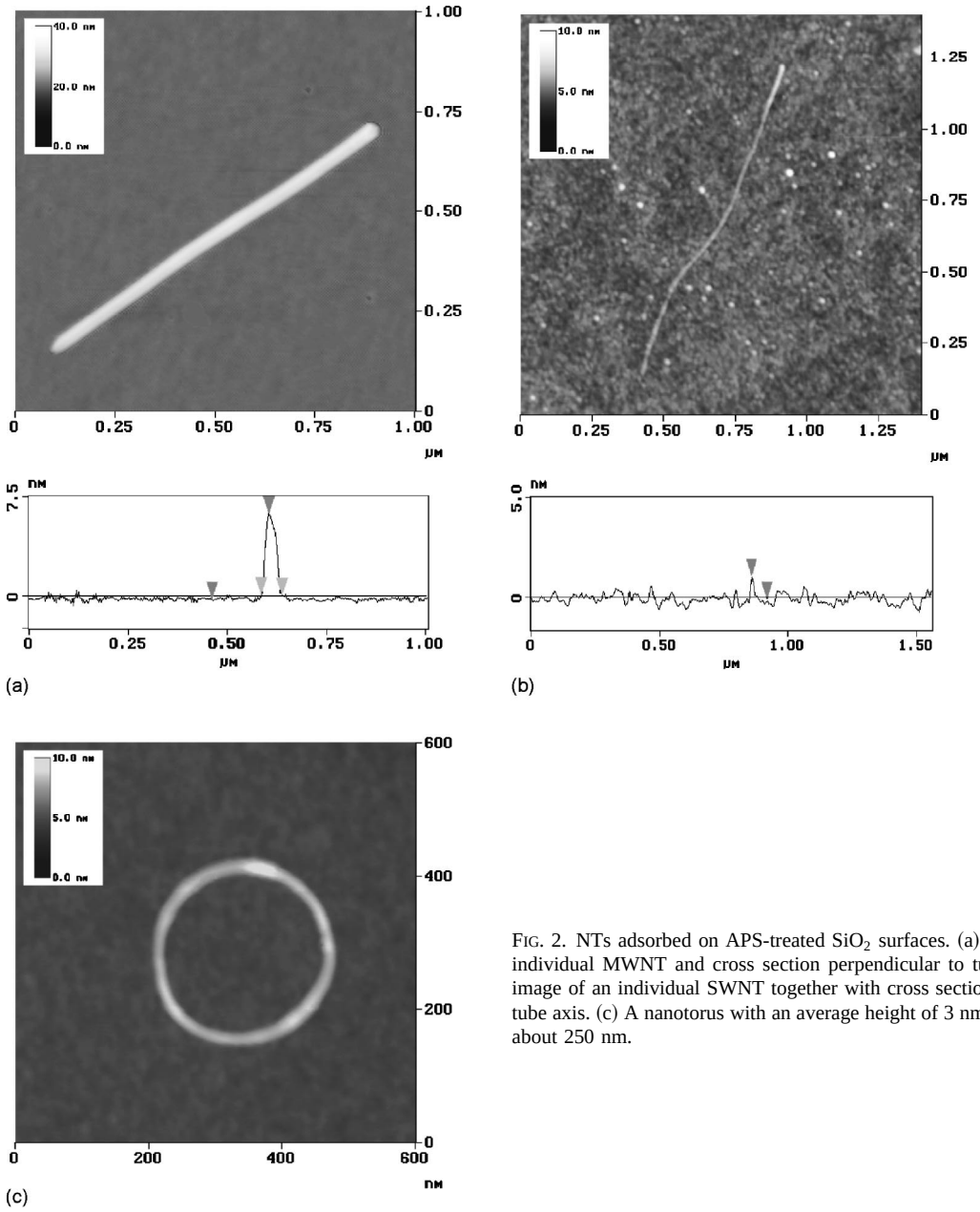

FIG. 2. NTs adsorbed on APS-treated SiO_2 surfaces. (a) SFM image of an individual MWNT and cross section perpendicular to tube axis. (b) SFM image of an individual SWNT together with cross section perpendicular to tube axis. (c) A nanotorus with an average height of 3 nm and a diameter of about 250 nm.

jects with heights between 0.8 and 2 nm as individual SWNTs, whereas heights ranging between 2 and 5 nm were attributed to ropes. However, it is important to recognize the limitation of this assignment for the case of a bundle consisting of two 1 nm tubes.

A large fraction of the SWNTs exhibited a curved shape, sometimes forming loops or semicircles. Occasionally, we observed NTs forming a nanotorus, i.e., a closed nanotube without any apparent beginning or end. In Fig. 2(c) such a nanotorus with a diameter of $\approx$250 nm is shown. From the measured height of 3 nm it is concluded that the present torus consists of a rope of SWNTs. However, due to the limited lateral resolution of SFM, it is not possible to strictly exclude the possibility that the torus is not fully closed. On the upper part of the torus, there is a slightly thicker part (height of 5 nm), which might be formed by a catalytic particle which is incorporated in the torus.

IV. BENDING BEHAVIOR OF NANOTUBES ON ELECTRODES

The SFM investigation of MWNTs deposited on electrode arrays revealed a noticeable bending of the tubes upon crossing the electrode lines. This behavior is exemplified in Fig. 3 by a MWNT with a length of 850 nm and a height of 8 nm. By assuming an inner tube diameter between 0.7 and 2 nm and a shell separation of 0.34 nm,[6] the number of shells is estimated to 8–10. The bending of the tube over the two

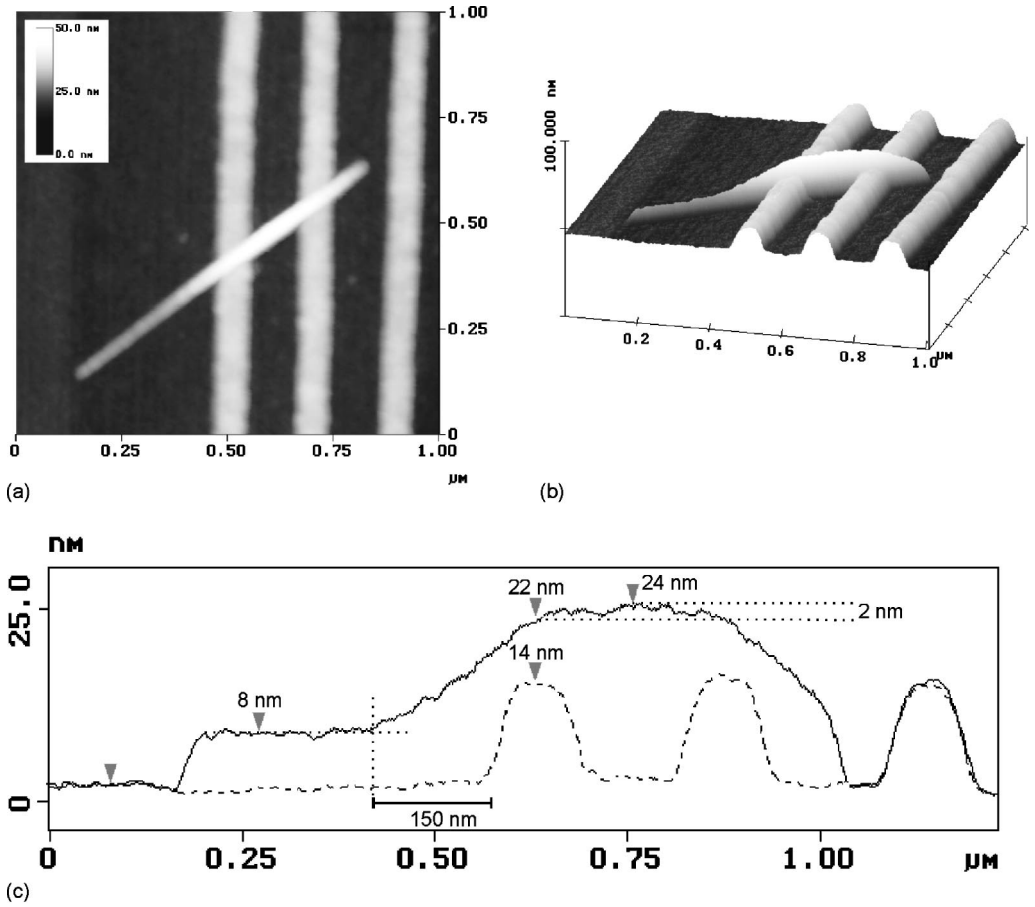

FIG. 3. SFM image of an individual MWNT bridging over two Au/Pd electrode lines: (a) Topographic view, (b) three-dimensional plot. (c) Cross section along tube axis (solid line), profile of underlying electrodes (broken line).

electrodes is stressed by the corresponding three-dimensional plot in Fig. 3(b). The electrode lines are 100 nm apart, 80 nm wide and 14 nm in height. A cross sectional view along the tube axis is given in Fig. 3(c) (full line), with the broken line representing the profile of the underlying electrodes. The slow rise of the profile of the NT over the electrodes starts about 150 nm in front of the left electrode line and is an indication of long range flexibility. The distance of the tube from the substrate has a maximum at about the middle of the electrode gap. Here, the top of the tube is 24 nm above the substrate. If one subtracts the electrode height of 14 nm and assumes a constant NT diameter of 8 nm, this leaves a surplus of 2 nm due to the convex bending. In contrast to the gradual rise in front of the left electrode, the descent after the right electrode is much more abrupt. This is ascribed to the ending of the tube at about 80 nm after crossing the electrode. We assume that on this side, the tube has a loose hanging end which makes no contact with the substrate.

A striking feature in the topographic image of Fig. 3(a) is that the tube width appears non-uniform. It seems to be increased between the electrodes, whereas it is of smaller, almost identical size on the electrodes and the wafer surface. The most likely explanation for this observation is an artifact due to tip convolution. In general, the degree of tip convolution depends on the effective height of the investigated object,[24] as illustrated in the scheme of Fig. 4. If the heightof the object is larger than the range over which the tip shape can be approximated as a sphere additional broadening will result. In the present case, this effect is more pronounced for

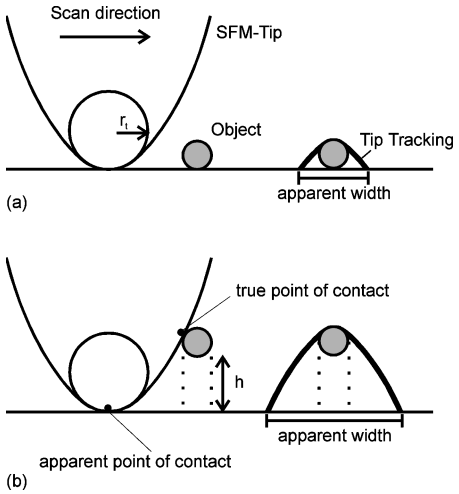

FIG. 4. Schematic representation of tip convolution, solid lines represent the tip tracking. (a) Due to the finite size of the SFM tip (tip radius r_t) the imaged object appears wider. (b) If the same object is located at a distance h above sample surface, it first gets in contact with the broadened upper part of the tip and will be imaged considerably wider in comparison to case (a).

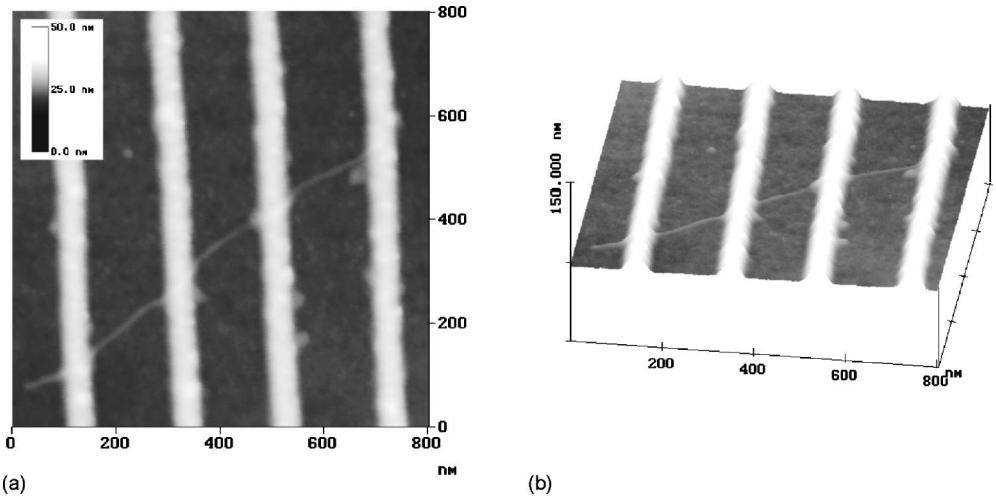

FIG. 5. SFM image of an individual SWNT deposited on an electrode array: (a) Topographic view and (b) three-dimensional plot.

the tube between the electrodes compared to the tube on the substrate or on the electrodes. Hence, the tube appears wider in the gap region (tube width ≈ 58 nm) than in the latter two regions (tube width ≈ 45 nm).

The tube bending over the electrode lines allows an estimate of the elasticity constants. In a first approach, the Young modulus of the MWNT in Fig. 3 was estimated by solving the classical beam elasticity equation[25] for a nanotube absorbed on a stepped surface:

$$\frac{d^4 f(z)}{d^4 z} = \frac{K(z)}{YI}, \tag{2}$$

where $f(z)$ measures the distance of the nanotube with respect to the planar surface, $K(z)$ is the load force per unit length as related to the nanotube/surface interaction, Y is the Young modulus, and I the moment of inertia of the cross sectional area. The attractive substrate/nanotube force per unit length was approximated by the van der Waals attraction.[26] The interaction between carbon and surface atoms is modulated by a Lennard-Jones potential $c/r^{12} - d/r^6$, where the attractive part is obtained within the Lifshitz theory of van der Waals forces. The values used in the present study are $c = 2.5 \times 10^4$ eV Å^{12} and $d = 27$ eV Å,[6] which are very similar to the C/C van der Waals interaction parameters.[27] The model is simplified by treating the substrate as a continuous medium. Under this assumption, the tube/substrate interaction per unit length becomes an analytical function.[26] This approach is similar to studies which use van der Waals interaction between carbon and graphite.[27,28]

We describe the surface through a step function of height h (the electrode height in the experiment). By using a finite-difference approximation to the fourth-order derivative and imposing that the tube is lying flat on the surface far from the step, Eq. (2) transforms to a matrix equation that can be solved. By least-squares fitting of the experimental data we found that a Young modulus of the order of 1 TPa reproduces the measured SFM profile reasonable well.[29] This range is in good accordance with previous experimental results[17,30] and the calculated Young moduli of MWNTs in the work of Lu.[12]

In contrast to the rather stiff MWNTs described above, SWNTs turned out to be highly flexible on a short length scale. Figure 5 shows an individual SWNT with a length of about 890 nm. The measured tube height of 1.2 nm is strong evidence for an individual single-walled tube. As apparent from Fig. 5(b), the tube starts to bend abruptly near the electrode edges. However, because of the irregular shape of the electrodes it is difficult to determine the distance from the electrode at which the tube begins to bend. It is roughly estimated to be 20 nm in front of the electrode, which is about one order of magnitude smaller than in the MWNT case of Fig. 3. Other investigated SWNTs crossing electrode lines exhibited a comparably high flexibility.

In Fig. 6, a larger scan of SWNTs (individual tubes and ropes) deposited on the electrode array is shown. The image

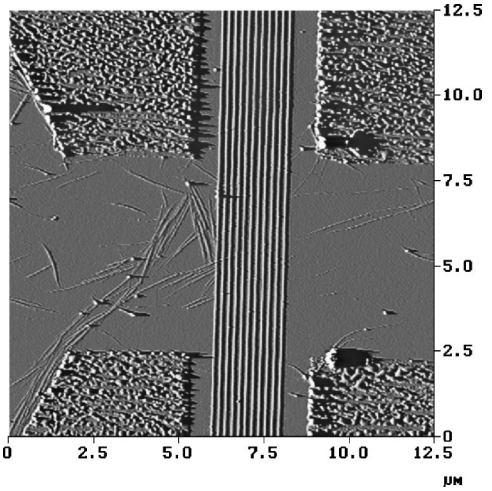

FIG. 6. SFM image of SWNTs (individual and ropes) deposited and flow oriented on an electrode array (the amplitude image of Tapping Mode is shown for clarity). NTs are adsorbed predominately on the left side of the electrode array.

displays eleven electrode lines surrounded by four large marker pads in the corners of the image. It is recognized that the NTs are (partially) aligned and adsorbed predominately on the left side of the electrode array. A similar result was observed for each of four other electrode arrays on the same substrate. We explain this observation by a flow effect during the rinse of the substrate after adsorption of the surfactant-stabilized NTs. Presumably the NTs adsorbed on the substrate surface are mobilized upon removal of the surfactant and flow against the electrode lines and markers, both of which act as mechanical barrier. This effect might be exploited for a controlled orientation of NTs on patterned surfaces.

V. CONCLUSIONS

It has been demonstrated by SFM investigations that NTs can be reproducibly adsorbed from surfactant-stabilized dispersions on chemically modified silicon oxide surfaces as well as on electrode arrays. During this process, effects such as flow orientation of the tubes which are usually not observed in deposition techniques like drying of suspensions or spin coating can occur. In addition, the SFM measurements reveal a substantially higher flexibility of SWNTs in comparison to MWNTs. These results are of importance for the investigation of the relationship between electrical transport through NTs and their structural and mechanical properties.

ACKNOWLEDGMENTS

This work was partially supported by the TMR program NAMITECH of the European Community and the Sonderforschungsbereich 329 (Molekulare Elektronik). The authors thank C. Journet and P. Bernier (University of Montpellier) for supplying single-walled nanotube samples. The help of U. Waizmann with SEM is appreciated.

[1]S. Iijima, Nature (London) **354**, 56 (1991).
[2]A. C. Dillon, K. M. Jones, T. A. Bekkedahl, C. H. Kiang, D. S. Bethune, and M. J. Heben, Nature (London) **386**, 377 (1997).
[3]W. A. de Heer, J.-M. Bonard, K. Fauth, A. Châtelain, L. Forró, and D. Ugarte, Adv. Mater. **9**, 87 (1997).
[4]L. Chico, V. H. Crespi, L. X. Benedict, S. G. Louie, and M. L. Cohen, Phys. Rev. Lett. **76**, 971 (1996).
[5]S. Saito, Science **278**, 77 (1997).
[6]M. S. Dresselhaus, G. Dresselhaus, and P. C. Eklund, *Science of Fullerenes and Carbon Nanotubes* (Academic, San Diego, 1996), p. 756.
[7]M. Bockrath, D. H. Cobden, P. L. McEuen, N. G. Chopra, A. Zettl, A. Thess, and R. E. Smalley, Science **275**, 1922 (1997).
[8]P. G. Collins, A. Zettl, H. Bando, A. Thess, and R. E. Smalley, Science **278**, 100 (1997).
[9]S. J. Tans, M. H. Devoret, H. Dai, A. Thess, R. E. Smalley, L. J. Geerligs, and C. Dekker, Nature (London) **386**, 474 (1997).
[10]B. I. Yakobson, C. J. Brabec, and J. Bernholc, Phys. Rev. Lett. **76**, 2511 (1996).
[11]S. Iijima, C. Brabec, A. Maiti, and J. Bernholc, J. Chem. Phys. **104**, 2089 (1996).
[12]J. P. Lu, Phys. Rev. Lett. **79**, 1297 (1997).
[13]P. Calvert, Nature (London) **357**, 365 (1992).
[14]H. Dai, J. H. Hafner, A. G. Rinzler, D. T. Colbert, and R. E. Smalley, Nature (London) **384**, 147 (1996).
[15]A. N. Broers, W. W. Molzen, J. J. Cuomo, and N. D. Wittels, Appl. Phys. Lett. **29**, 596 (1976).
[16]M. R. Falvo, G. J. Clary, R. M. Taylor II, V. Chi, F. P. Brooks, Jr., S. Washburn, and R. Superfine, Nature (London) **389**, 582 (1997).
[17]E. W. Wong, P. E. Sheehan, and C. M. Lieber, Science **277**, 1971 (1997).
[18]G. S. Duesberg, M. Burghard, J. Muster, G. Philipp, and S. Roth, Chem. Commun. **1998**, 435 (1998).
[19]T. W. Ebbesen and P. M. Ajayan, Nature (London) **358**, 220 (1992).
[20]C. Journet, W. K. Maser, P. Bernier, A. Loiseau, M. Lamy de la Chapelle, S. Lefrant, P. Deniard, R. Lee, and J. E. Fischer, Nature (London) **388**, 756 (1997).
[21]M. Burghard, G. Duesberg, G. Philipp, J. Muster, and S. Roth, Adv. Mater. **10**, 584 (1998).
[22]As the interaction between tip and sample is nonlinear, the right term would be ''dilation'' rather than ''convolution'' [see J. S. Villarrubia, Surf. Sci. **321**, 287 (1994)].
[23]C. T. Gibson, G. S. Watson, and S. Myhra, Scanning **19**, 564 (1997).
[24]J. E. Griffith and D. A. Grigg, J. Appl. Phys. **74**, R83 (1993).
[25]R. P. Feynman, R. B. Leighton, and M. Sands, *The Feynman Lectures on Physics—Volume II* (Addison–Wesley, Palo Alto, 1966).
[26]J. N. Israelachvili, *Intermolecular and Surface Forces* (Academic, London, UK, 1995).
[27]L. P. Biró, S. Lazarescu, P. Lambin, P. A. Thiry, A. Fonseca, J. B.Nagy, and A. A. Lucas, Phys. Rev. B **56**, 12490 (1997).
[28]P. Lambin, V. Meunier, and L. P. Biró, Carbon (in press).
[29]A. Rubio, E. Hernández, J. Muster, G. S. Duesberg, M. Burghard, and S. Roth (unpublished).
[30]M. M. J. Treacy, T. W. Ebbesen, and J. M. Gibson, Nature (London) **381**, 678 (1996).